Surface Reconstruction Method for Multi-view Corneal Topography

Zoltán Fazekas[1], Alexandros Soumelidis[1], András Bódis-Szomorú[2], Ferenc Schipp[3], Béla Csákány[4], and János Németh[4]

[1] Computer and Automation Research Institute, Budapest, Hungary
{zfazekas,soumelidis}@sztaki.hu
[2] Department of Measurement and Information Systems, Budapest University of Technology and Economics, Budapest, Hungary
bodis@mit.bme.hu
[3] Department of Numerical Analysis, Eötvös Loránd University, Budapest, Hungary
schipp@ludens.elte.hu
[4] Department of Ophthalmology, Semmelweis University, Budapest, Hungary
{cb,nj}@szem1.sote.hu

Abstract. Our recently published specular surface reconstruction method developed for and used in an experimental multi-camera corneal topographer arrangement is summarized here for the colleagues attending the 7th Conference of the Hungarian Association for Image Processing and Pattern Recognition.

1 Introduction

The *cornea* is the primary optical structure that focuses the light entering the human eye. Particularly, its *outer surface* generates about the 70% of the total refractive power of the human eye; while other structures in the light-path – including also the crystalline lens – have smaller refractive power. It should be noted that the outer corneal surface itself is not an optical surface. It is the coating of this surface – called the *pre-corneal tear film* – that provides an optical surface; the film is replenished with every blink, and after its build-up, it provides a smooth optical surface on the microscopically irregular corneal surface. It is partly for the mentioned high percentage within the total refractive power that the detailed topographic characterization of the corneal surface has considerable diagnostic value. Examination devices and methods aiming at determining the corneal shape and using it for further optical calculations have a relatively long history. See for example [3] for the bibliographical details of papers written by Helmholtz, Placido and Gullstrand in the 19th century.

Today, *corneal topographers* are used in a wide range of ophthalmic examinations [2]. The majority of the measurement methods used in corneal topographers rely on the specularity of the cornea, or more precisely, that of the pre-corneal

⋆ Major part of this paper was published in [13].

tear-film. These methods are referred as reflection-based methods, and the topographers using these methods as *reflection-based topographers*. In case of such topographers, a bright measurement-pattern of known and well-defined geometry – e.g., concentric rings called in this context Placido-rings – is generated and displayed in front of the patient's cornea. The reflection of this pattern at the pre-corneal tear-film is photographed by one or more camera. The distorted virtual image, or images are then analyzed, and the corneal surface is mathematically reconstructed. Based on this reconstruction, height- and refractive power-maps are produced and displayed for inspection by the ophthalmologist. In case of healthy and regular corneal surfaces, the presently available corneal topographers generally produce good quality corneal snapshots, and based on these, precise and reliable maps are generated. However, even for healthy regular surfaces, small impurities and tiny discontinuities in the pre-corneal tear-film may produce extensive measurement errors.

Fig. 1. Binarized image of a reflected Placido ring pattern taken by an existing corneal topographer. The skipped and uncorrected ring-points form a wedge-shaped artifact in the ring-pattern. Its effect on the optical power map is shown in Fig. 2

.

Fig. 2. The effect of the ring-detection anomaly on the optical power map. The wedge-shape artifact in Fig. 1 result in a region with low optical power.

Such a measurement anomaly is shown in Fig. 1, while its corresponding refractive power map is shown in Fig. 2. Missed ring-points result in rings with high curvature-variance near these misses. Such rings in turn result in significant and extensive, i.e., non-local errors in the generated optical power map.

The measurement anomalies are even greater, if callused, irregular corneal surfaces are examined using a Placido-based topographer [11]. In this case, many of the reflected ring-points disappear and it is difficult, if at all possible, to determine the original radial order of the ring-segments. See Fig. 3 for such a problematic case. Consequently, only a partial, rough and very unstable surface reconstruction can be achieved that is of no use for any diagnostic purposes.

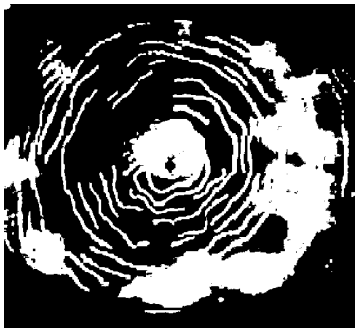

Fig. 3. Binarised version of a distorted and fragmented Placido ring system that had been recorded for a callused, irregular corneal surface.

It is particularly the case, when simplistic measurement-patterns, such as the one mentioned above, are used. To this end, several more informative measurement-patterns were suggested recently. These patterns facilitate the identification of point-correspondences by using location-dependent color-coding, e.g., [12].

2 Reconstruction of Smooth Specular Surfaces

The mathematical reconstruction of smooth specular surfaces from the distortion they cause to some known pattern – when the pattern is viewed, or photographed as being reflected from the mentioned surface – is an active research area. The reconstruction can be local or global. In case of *local reconstruction*, sufficient conditions are given for the uniqueness of a local surface reconstructions in [6]. Also, the formulae to determine the actual surface-patch are given there. Methods for the practically more important *global reconstruction* are published in [7], [10]. Each of these methods relies on the *smoothness of the surface* to be reconstructed and uses *several views* to make the unique reconstruction possible. For an unknown smooth, convex specular surface – viewed by several cameras – those points are located on or near to the specular surface for which the unit normal vectors – calculated from the real or assumed reflections at these points – are approximately the same for different views. This observation is the basis of the *voxel-carving method* suggested by [7]. Clearly, this method can be used only for those surface portions that reflect the measurement-pattern into more

than one camera. An elegant surface reconstruction method was proposed by [10]. There the light-reflection at the surface is described with a *total differential equation* (TDE). The mathematical reconstruction of the surface is achieved by the numerical solution of this TDE.

3 The Proposed Reconstruction Method and the Arrangement Used as the Testbed for the Method

The surface reconstruction method proposed in [13] and summarized here was developed for an experimental corneal topographer arrangement used as a test-bed. Hereafter, this arrangement will be referred as *target-arrangement*. Its camera-system comprises three cameras. The *camera-system*, together with the *measurement-pattern generator* (i.e., a high-quality TFT-display) is shown in Fig. 4.

Fig. 4. The camera system of the multi-camera corneal topographer arrangement.

Note that the target-arrangement and its hardware were described in more detail in [12]. It should be underlined that the surface reconstruction method derived for the target-arrangement is *applicable to most multi-camera arrangements* that are reasonable in the given application.

Image Segmentation and Filtering. A rectangular array of bright circular spots was used as *measurement-pattern*. The reflected blobs – corresponding to the circular spots in the rectangular array of the measurement-pattern – were detected at a number of thresholds, and the center-point and a few shape-descriptors were calculated for each blob. Such a corneal reflection image is shown in Fig. 5, while in Fig. 6, the spots detected with the mentioned thresholds are shown as circular blobs.

The detected blobs were then checked for their areas, axis-lengths and their orientation. Blobs being relatively close to each other and having similar shape-descriptor values were united, as these were assumed to be the images of the

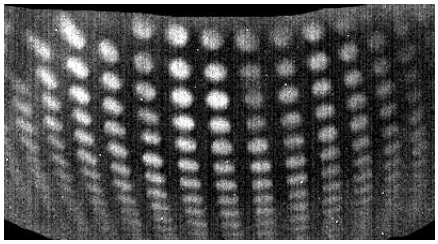

Fig. 5. A corneal reflection image.

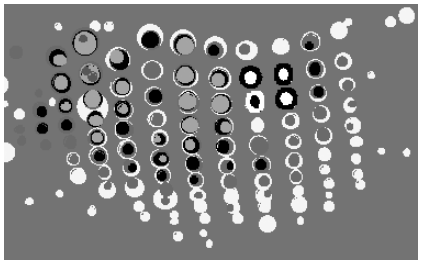

Fig. 6. The blobs detected – marked here as disks – in the reflection image of Fig. 5

same circular spot. Blobs with much bigger areas than those of the nearby blobs were removed, as these were assumed to be segmentation artifacts.

Blob Identification. A colored disk – discernible with some effort in Fig. 5 – was used for *marking the center of the rectangular array*. The corresponding blobs in the three reflection images were identified and their center-points were used as reference and starting points for the subsequent blob-identification process. Each of the three 2D-point-sets – formed by the blob-centers of the blobs detected in the reflection images – were submitted to *Delaunnay-triangulation*. The sides of the resulting triangles were then tracked starting from the aforementioned reference points in *"row" and "column" directions*. Based on the tracking results, correspondences (i.e., mapping) between the original circular spots and the detected blobs were established. For the purpose of the tracking the side-lengths of the Delaunnay-triangles, the directions of sides and the area-ratio of the blobs concerned were used.

Approximation of the Apparent Distortions. *Spline interpolation* was used to convert the three discrete mappings to continuous mappings, thereby approximating the optical mappings (distortions) between the points of the measurement-pattern and those of the reflection images. Such a spline interpolation i.e., a mesh of splines, is shown for a corneal surface in Fig. 7.

Mathematical Model of the Light-reflection at the Specular Surface. Mathematically, the *smooth specular convex surface* F is described and sought

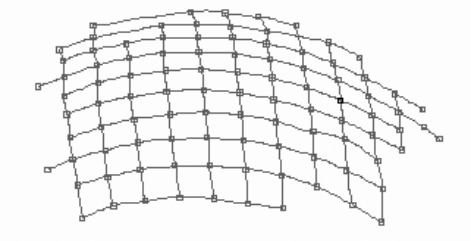

Fig. 7. Spline interpolation between the detected blob-centers.

in preferably chosen spatial coordinate systems. Each of these coordinate systems corresponds to one of the cameras of the topographer arrangement. (For notational simplicity, only one of these coordinate system is considered in the following formulae.) The origin of the *camera coordinate system* B is placed in the optical center of the particular camera and the z-axis of this coordinate system is the optical axis BB' of the camera. The specular surface F, i.e., the surface of an artificial or a real cornea is described in the following form:

$$F(x_1, x_2) = S(x_1, x_2)\hat{x} \qquad (\hat{x} = (x_1, x_2, 1)^T) \tag{1}$$

Here, $S(x)$ $(x = (x_1, x_2))$ is a scalar-factor describing the *inverse distance-ratio*, measured from B, of the 3D point P_x – corresponding to $\hat{x}$ – and the surface-point appearing in the same direction as P_x from B.

The *propagation of light* from the points of the measurement pattern to those of the (distorted) image, i.e., $P_y P P_x$, is described in the coordinate system. By doing so, a mapping is identified between the points P_y of the measurement pattern and the points P_x of the image: $P_y \to P_x$. It follows from the conditions prescribed for the mathematical surface that mapping $P_y \to P_x$ is one-to-one.

It follows from the *physical law of light-reflection*, the two-variable function $S(x)$ describing surface F satisfies the following *first-order partial differential equation* (PDE):

$$\frac{1}{S(x)}\frac{\partial S(x)}{\partial x_j} = \frac{v_j(x) - x_j}{\langle \hat{x}, \hat{x} - v(x) \rangle} \qquad (j = 1, 2), \tag{2}$$

where

$$v(x) = |\hat{x}\,| \frac{k + f(x) - S(x)\hat{x}}{|k + f(x) - S(x)\hat{x}|} \tag{3}$$

and function $f(x)$ can be expressed with mapping $P_x \to P_y$. Here, k is a vector pointing to a reference point in the plane of the measurement pattern; while $\langle ., . \rangle$ denotes the scalar product of the 3D space. It follows from the mathematical model described above that surface F can be determined uniquely under the *starting condition* of $S(0, 0) = s_0$, if the $P_y \to P_x$ mapping is known.

Using Stereo Information for Determining the Starting Condition. The exact value of the above starting condition could be found out by including two laser-lights for each camera (as done in other topographers). However, this distance setting mechanism is unnecessary here, as precise stereo information can be gathered with *two calibrated cameras* looking at the *same patch* of specular surface. An *assumed surface-point* and the *unit normal vector* at this point – determined from the first reflection image – are used to determine the point in the measurement-pattern that should be seen in the second image. The Euclidean distance between the *"should-be-seen" point* and the *point really seen* by the second camera is calculated. If this distance is significant for an assumed surface-point, then it is – in reality – off the surface. By moving along possible surface-points and considering also their unit normal vectors that are viable for the first camera, the aforementioned distance must be minimized. The near-zero valued minima mark the spatial positions of surface-points that can be used as stating points for the reconstruction.

Individual and Joint Camera Calibration. In the processing steps outlined above, it was tacitly assumed that the cameras in the arrangement were calibrated. To satisfy this assumption, the *chessboard-based calibration approach* described in [4] was used. A free MATLAB-implementation is available on the web and is described in [14]. This implementation, however, is difficult to handle, and useful *restrictions on camera-parameters* cannot be easily imposed. For these reasons, a new implementation of the above calibration approach was developed and used.

For the reported topographer arrangement, a 10mm by 10mm chessboard was used as *fiducial*. Firstly, it was placed in an approximately horizontal position and was photographed. The calibration step is shown in Fig. 8. Then the fiducial was fixed onto a *wedge* and was turned around an axis, which was more or less perpendicular to the measurement-pattern's plane. See Fig. 9.

The fiducial was photographed in a number of positions, then the above camera calibration procedure was carried out for each camera. The plane-positions recovered in the calibration process were as expected, however, it soon turned out that the calibration of the multi-camera arrangement – based on these individual camera calibrations only – does not ensure the precision required for the surface reconstruction.

Therefore, a second – fine-tuning – calibration step was necessary; *a joint calibration of the cameras* in the topographer arrangement had to be carried out. The simulation programs developed for modelling reflections of smooth specular surfaces turned out handy for this purpose. A *spherical artificial cornea with know radius* was used as a fiducial in this case.

An *optimization procedure* was carried out with respect to the position of the artificial cornea and the external camera-parameters of the cameras in the arrangement, the aim was to minimize the total sum of quadratic error between the blob-centers in the simulated reflection images and the detected ones. The

optimization resulted in *significant point position-changes* in the measurement-pattern's plane.

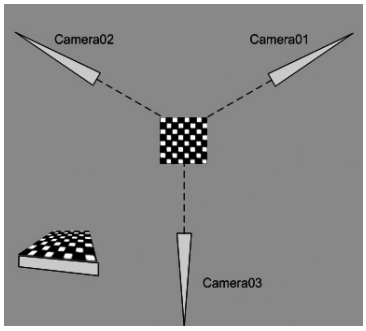

Fig. 8. Setting a common reference point for the three cameras.

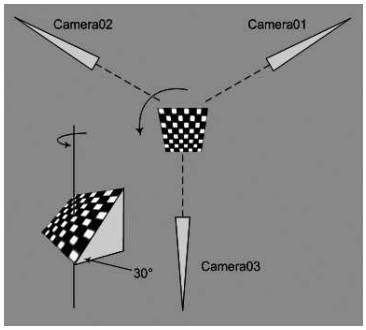

Fig. 9. The checkered wedge used for calibrating the individual cameras.

The Surface Reconstruction Procedure. A numerical procedure was devised to solve the above PDE's. The solution of these PDE's in effect conveys the reconstructed corneal surface. The solution involves *transcribing the PDE's for the "row" and the "column" directions.*

In this manner, *first-order ordinary non-linear differential equations* were generated. These were then numerically integrated – using the well-known *Runge-Kutta method* – along "row" and "column" directions, as necessary.

The *starting conditions* were derived with the method outlined earlier. A efficient computational scheme was devised to re-use the points computed earlier to improve reconstruction speed. In Figs. 5, 6, 7 and 10, the main stages of the reconstruction process can be followed for a living cornea.

4 Conclusion and Future Work

The majority of the topographers in use today, rely on *one view only*, which is *theoretically insufficient* for the unique reconstruction of the corneal surface.

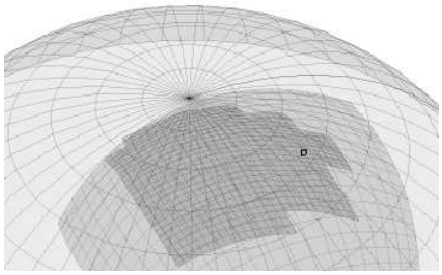

Fig. 10. A surface region reconstructed from one of the camera-views.

To overcome this *essential measurement deficiency*, a *multi-camera arrangement* was proposed by the authors and *mathematical methods* were devised for the specular surface reconstruction. However, further experiments and simulations are required to *improve the surface coverage* of the multi-camera arrangement.

Acknowledgments. This research has been partially supported by the *National Office for Research and Technology (NORT), Hungary,* in the frame of the NKFP-2/020/04 research contract.

References

1. Halstead, M. A., Barsky, B. A., Klein, S. A., Mandell, R. B.: Reconstructing Curved Surfaces from Specular Reflection Patterns Using Spline Surface Fitting to Normals. In: 1ACM SIGGRAPH, ACM (1996)
2. Corbett, M. C., Rosen, E. S., O'Brart, D. P. S.: Corneal Topography: Principles and Practice. Bmj Publ. Group, London, UK (1999).
3. Jongsma, F., de Brabander, J., Hendrikse, F.: Review and Classification of Corneal Topographers. Lasers in Medical Science, vol. 14, pp. 2–19 (1999)
4. Zhang, Z.: A Flexible New Technique for Camera Calibration. IEEE Transactions on Pattern Analysis and Machine Intelligence, vol. 22, no. 11, 1330–1334 (2000)
5. Savarese, S., Chen, M., Perona, P.: Second Order Local Analysis for 3d Reconstruction of Specular Surfaces. Proceedings of the First Int. Symposium on 3D Data Processing Visualisation and Transmission, IEEE, (2002)
6. Savarese, S., Perona, P.: Local Analysis for 3d Reconstruction of Specular Surfaces - Part II. In: Proceedings of the 7th European Conference on Computer Vision, LNCS, vol. 2351, pp. 1148–1158. Springer, Heidelberg (2002)
7. Bonfort, T., Sturm, P.: Voxel Carving for Specular Surfaces. In: 9th IEEE Conference on Computer Vision, vol. 2 (2003)
8. Savarese, S., Chen, M., and Perona, P.,: What Do Reflections Tell Us About the Shape of a Mirror? In: Applied Perception in Graphics and Visualization, ACM SIGGRAPH, ACM (2004)
9. Fleming, R. W., Torralba, A., Adelson, E. H.: Specular Reflections and the Perception of Shape. Journal of Vision, 798–820 (2004)

10. Kickingereder, R. Donner, K,: Stereo Vision on Specular Surfaces. In: Proceedings of the 4th IASTED International Conference on Visualization, Imaging, and Image Processing, IASTED (2004)
11. Erdélyi, B., Németh, J.: Atlas of the Difficult-to-Measure Corneal Surfaces. In Research Report of the Cornea Consortium, No. CORNEA-EXT-1M09. SZTAKI, Budapest, Hungary (2005)
12. Soumelidis, A., Fazekas, Z., Schipp, F., Edelmayer, A., Németh, J., Csákány, B.: Development of a Multi-camera Corneal Topographer Using an Embedded Computing Approach. In: Proceedings of the First Int. Conference on Biomedical Electronics and Devices, pp. 126–129. Funchal, Madeira, Portugal (2008)
13. Fazekas, Z., Soumelidis, A., Bódis-Szomorú, A., Schipp, F.,: Specular Surface Reconstruction for Multi-camera Corneal Topographer Arrangements. In: 30th Annual International IEEE EMBS Conference, pp. 2254–2257, Vancouver, British Columbia, Canada (2008)
14. Bouguet, J.-Y.: Camera Calibration Toolbox for MATLAB. California Institute of Technology (2007)